Journal of Environmental Chemical Engineering 10 (2022) 108320

Contents lists available at ScienceDirect

Journal of Environmental Chemical Engineering

journal homepage: www.elsevier.com/locate/jece

TACN-Mn catalyst use in an advanced oxidation process for efficient micropollutant abatement in wastewater: A transformation study of diclofenac and sulfamethoxazole

Julia Wolters [a], Muhammad Usman [a], Johanna Mathiä [a], Dirk Dirichs [a], Daniel Bastian [a], Benedikt Aumeier [a], Carsten Bolm [b], Volker Linnemann [a], Thomas Wintgens [a,*]

[a] Institute of Environmental Engineering (ISA), RWTH Aachen University, Mies-van-der-Rohe-Str. 1, 52074 Aachen, Germany
[b] Institute of Organic Chemistry (IOC), RWTH Aachen University, Landoltweg 1, 52056 Aachen, Germany

ARTICLE INFO

Editor: Dr. G. Palmisano

Keywords:
Degradation
Kinetics
Matrix
Trace substances
Transformation products

ABSTRACT

Advanced oxidation processes (AOP) are key technologies that can degrade micropollutants in wastewater treatment. In this study, we examined how well the TACN-Mn catalyst can be applied in environmentally relevant conditions (ambient temperature and near-neutral pH) in combination with hydrogen peroxide (H_2O_2). Furthermore, we investigated the degradation – including the reaction pathways, kinetics and transformation products (TPs) – of the two relevant micropollutants, diclofenac (DCF) and sulfamethoxazole (SMX), in two different water matrices. The rate constants we identified compared well to literature data and showed a strong pH dependency: The pseudo first-order rate constants for DCF degradation in ultrapure water varied from 4.45×10^{-3} min^{-1} to 1.06×10^{-1} min^{-1} when the pH was increased from 7.5 to 9.0, and for SMX degradation, the rate constants ranged from 1.62×10^{-3} min^{-1} to 2.33×10^{-2} min^{-1}. In wastewater, the oxidation was still effective, but at a lower rate and to a lesser extent than that in ultrapure water. TPs and reaction pathways of DCF and SMX were elucidated by LC-HRMS. TPs formed were very similar to those reported in previous studies about reactions with OH radicals. These promising results are the prerequisites for further investigations to optimize and evaluate the TACN-Mn/H_2O_2-AOP.

1. Introduction

Since organic micropollutants are not completely removed from municipal wastewater in conventional treatment plants, the remaining micropollutants enter the aquatic environment via the receiving water. They may pose a risk to humans and the environment and, therefore, are monitored and increasingly regulated by authorities. Expected regulations regarding advanced wastewater treatment to address micropollutants have led to extensive research towards possible treatment processes, including advanced oxidation processes (AOP). In general, AOPs are used to generate highly reactive species when an oxidant is activated in some form. These AOPs include various physical, electrochemical and catalytic processes, and some of them involve the use of energy-intensive UV radiation or chemicals, like hydrogen peroxide (H_2O_2). H_2O_2 is an inexpensive and environmentally friendly oxidizing agent [1]. Since it is usually not reactive enough below 80 °C, catalytic activation is necessary [1,2]. In this context, metal complexes have been investigated as possible catalysts, whereby manganese complexes have proven to be more environmentally friendly than most other transition metal species [1]. Manganese-1,4,7-trimethyl-1,4,7-triazacyclononan (TACN-Mn) is such a metal complex and characterized by the fact that the manganese can reversibly adapt to different oxidation states without being separated from the complex. TACN-Mn was originally used as a bleaching catalyst in detergents [2]. It is known as a versatile catalyst for the oxidation of a large number of organic functional groups by the oxidizing agent H_2O_2 [1]. The structure of TACN-Mn is shown in Fig. 1.

A special feature of the process with TACN-Mn and H_2O_2 is that, unlike most AOPs, high-valent manganese species are the active oxidizing agent in the system [1,3]. The exact nature of this reactive species is unknown, but a mononuclear oxo-manganese (V) species is

* Corresponding author.
E-mail addresses: wolters@isa.rwth-aachen.de (J. Wolters), usman@isa.rwth-aachen.de (M. Usman), johanna.mathiae@rwth-aachen.de (J. Mathiä), dirk.dirchs@rwth-aachen.de (D. Dirichs), bastian@fiw.rwth-aachen.de (D. Bastian), aumeier@isa.rwth-aachen.de (B. Aumeier), carsten.bolm@oc.rwth-aachen.de (C. Bolm), linnemann@isa.rwth-aachen.de (V. Linnemann), wintgens@isa.rwth-aachen.de (T. Wintgens).

https://doi.org/10.1016/j.jece.2022.108320
Received 21 April 2022; Received in revised form 18 July 2022; Accepted 21 July 2022
Available online 22 July 2022

suspected to be the active oxidizing agent [1–3]. Depending on the target substance investigated, different oxidation mechanisms by the system TACN-Mn/H_2O_2 are suggested in the literature [3,4]. To the best of our knowledge, no scientific publication could be found in which the oxidation of drugs by this system was described in detail. Therefore, it is only possible to make assumptions about the reaction mechanism taking place there. Since the epoxidation of alkenes is also oxidation, apart from the actual oxidation, no further reactions occur between the alkenes and the TACN-Mn. The epoxidation of cinnamic acid is chosen at this point as a possible reaction mechanism in the oxidation of pharmaceuticals and other organic pollutants [1,3]. In past studies, the reaction mechanism was illustrated by the epoxidation of cinnamic acid [1,3]. Fig. 2 shows the modified reaction mechanism of the TACN-Mn/H_2O_2 system for our application [1,3].

The dinuclear manganese complex is reductively cleaved in the first step of the effect mechanism, creating mononuclear manganese (IV) species. In water, they can exist in the two forms shown. A one-electron reduction of the Mn (IV) complex by H_2O_2 then takes place, which results in an HO_2 radical and a Mn (III) complex. This complex is then oxidized by H_2O_2 to Mn (V) species, which are the active oxidizing agents in the process. By reacting with organic pollutants and oxidizing them, Mn (V) species are reduced to the Mn (III) complex again. Depending on the oxidized substance, oxidation can take place through an electron or an oxygen transfer [1,2]. Alternatively, the Mn (V) complex can be reduced back to the Mn (IV) species by a renewed attack by H_2O_2. As explained above, TACN-Mn has already been used in various applications (e.g. detergents) and is known for strong performance, especially at high temperatures and high pH [5].

The use of TACN-Mn as a catalyst for H_2O_2 as an AOP in wastewater treatment, especially in the area of municipal wastewater treatment, has not yet been covered in detail. In 2009, Unilever applied for a patent for a wastewater treatment process using H_2O_2 and a TACN-Mn-based catalyst. The background of the application is the treatment of industrial wastewater. This includes wastewater streams with paint contamination, high biochemical oxygen demand (BOD_5) or chemical oxygen demand (COD), chlorinated phenolic ingredients, pharmaceutical ingredients, quinones, azo-containing molecules, alkenes, alcohols, and sulfur-containing compounds [6]. Regarding the patent, the catalyst has only been used in combination with electrochemical activation, which was not done here. Moreover, our study is the first one investigating the performance of TACN-Mn/H_2O_2 in a municipal wastewater matrix and the degradation of particularly relevant substances in this field. In municipal wastewater treatment, the use of an AOP based on TACN-Mn and H_2O_2 can be compared with other AOPs that also use chemical catalysts. The Fenton process and Fenton-like processes can be used for comparison, e.g. in terms of operational parameters to be set.

This study aims to investigate if TACN-Mn in combination with H_2O_2 can be used for advanced wastewater treatment as a possible extended application. Experiments were carried out to check if the AOP catalyst works at environmentally relevant conditions (ambient temperature and near-neutral pH) and degrades micropollutants present in effluents of municipal wastewater treatment plants. During AOP, highly reactive species cause a fast reaction with organic substances. This reaction may lead to biodegradable substances and mineralization, but also to the formation of transformation products (TPs) which may be more or less persistent and more or less toxic than the parent compound. In this study, the reaction pathways and kinetics of two widespread model micropollutants – diclofenac (DCF) and sulfamethoxazole (SMX) – will be elucidated and possible reaction mechanisms suggested.

2. Material and methods

2.1. Chemicals and reagents

TACN-Mn {Dragon PF6 – [bis(N,N',N"-trimethyl-1,4,7-triazacyclononane)-trioxodimanga-nese (IV) di(hexafluorophosphate) monohydrate] was provided by Catexel in powder form and was dissolved in ultrapure water before the experiment. H_2O_2 (30%) was purchased from Merck (Darmstadt, Germany). Sodium hydroxide and sulphuric acid from Bernd Kraft GmbH (Germany) were used for pH adjustment. Standards for DCF and SMX were obtained in the highest available purity from Sigma Aldrich (Darmstadt, Germany). Stock solutions were prepared in methanol. All solvents (water, methanol, acetonitrile) were of the highest purity and were purchased from VWR (Darmstadt, Germany). Formic acid was used as a modifier and obtained from Fisher Scientific (Dreieich, Germany). Methylene blue from Riedel-de Haën (Seelze, Germany) was used as a model substance for additional orienting experiments.

2.2. Sample preparation for identification of transformation products

To stop the further formation of TPs after samples were taken, those containing DCF were mixed with a 1.5 mol amount of sodium sulphite to scavenge free OH radicals. Samples containing SMX were mixed with catalase (Micrococcus lysodeikticus, 111700 U/mL, Sigma-Aldrich) respectively. Background concentrations of DCF and SMX in the wastewater sample (100 mL) were measured after being enriched by Oasis HLB (60 mg, 3cc) and eluted by 3 mL MeOH.

2.3. Analysis by LC-HRMS

TPs were analyzed with an Orbitrap ID-X (Thermo Scientific, USA) equipped with a Vanquish UHPLC system consisting of a binary pump and split sampler HT and a heated ESI ion source. Separation was performed on a Hypersil Gold aQ (150 mm, 2.0 mm, 5 μm) from Thermo Fisher (USA) and kept at 40 °C. The mobile phase consists of Eluent A (0.1% formic acid in water) and Eluent B (0.1% formic acid in MeOH). The injection volume was 10 μL at a flow rate of 0.3 mL/min. Gradient

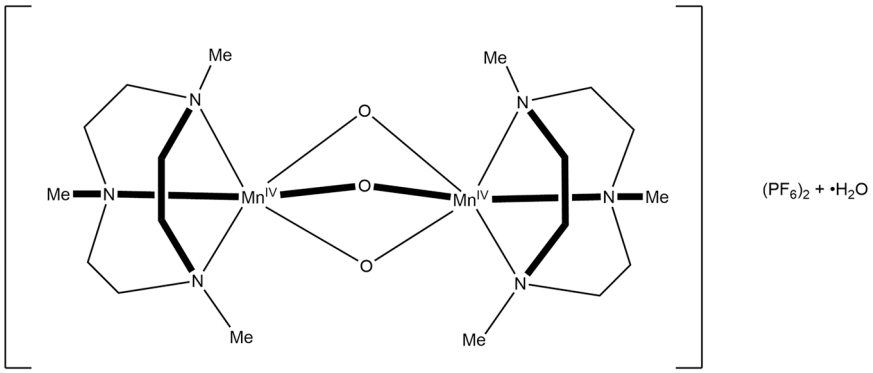

Fig. 1. Structure of TACN-Mn [1].

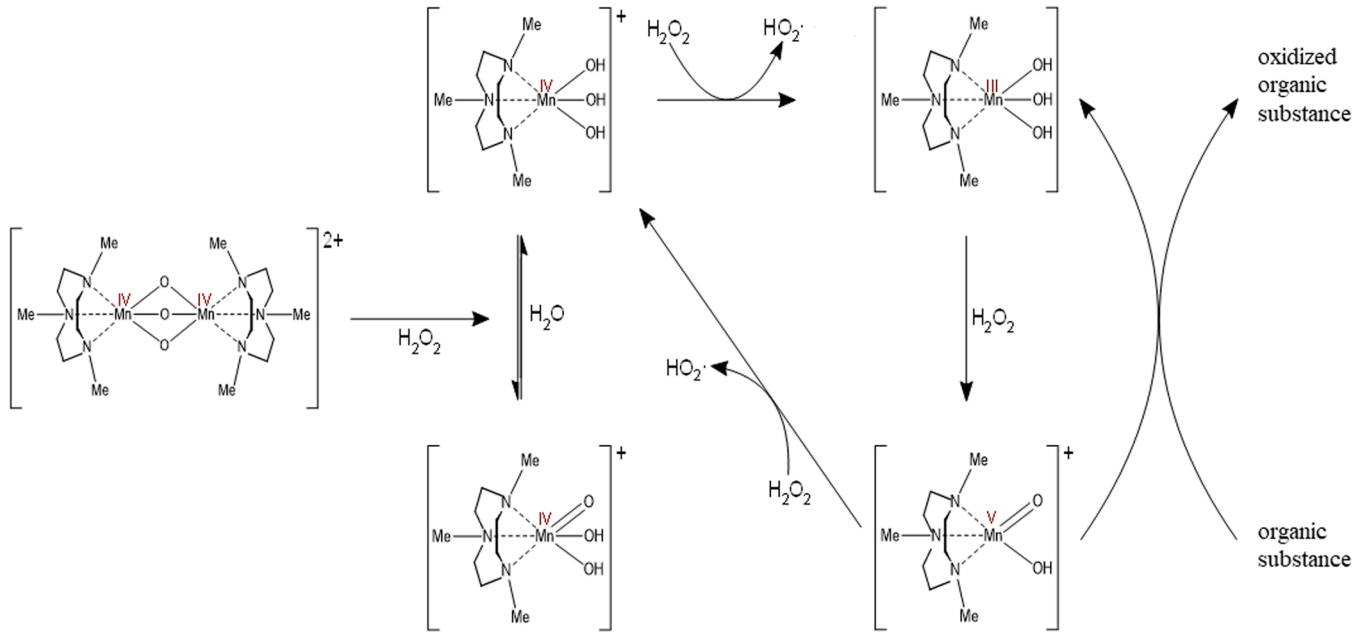

Fig. 2. Effect mechanism of the system TACN-Mn/H_2O_2 modified from GILBERT et al. [3] and LINDSAY SMITH et al. [1].

elution was performed from 98% A to 2% A over 27 min. Data-dependent acquisition was performed in ESI+ and ESI- modes with both collision-induced dissociation (CID) at 30% fixed collision energies and high-collisional dissociation (HCD) using assisted collision stepped collision energies of 40%, 50%, and 60%. The mass resolution of the orbitrap analyzer was 120,000.

Data analysis and instrumental control were done by Tracefinder 5.0, XCalibur, and Compound Discoverer 3.2. Retention time (RT) alignment and background subtraction were done by Compound Discoverer 3.2. Filling water was used as blank for background subtraction, which is performed by the software when features are also identified in the blanks. Suspected TPs from different AOP experiments were summarized in a list, and the exact masses were added as a mass list in Compound Discoverer 3.2. Identification of unknown or suspect TPs was verified again by a visual comparison of the experimental spectrum against the recommended library spectrum and the calculated total score of Compound Discoverer 3.2 software. These features were further sorted out using at least three associated fragment ions with a mass accuracy below 5 ppm.

2.4. Analysis by IC

Oxyhalides chlorite, chlorate and bromate were investigated as potential inorganic transformation products. Chlorite and chlorate were determined by an ion chromatographic (IC) system (Metrohm Ltd., Switzerland) with chemical suppression and a Metrohm 732 conductivity detector. Bromate was determined using post-column reaction (PCR - Tri-iodide method) according to DIN EN ISO 11206. The analytical column used for the anion separation was a universal anion column Metrosep A Supp 16 (4.0 mm × 150 mm; Altech, USA), and the injection volume was 20 µL (1000 µL for bromate analysis). Eluent was a 3.6 mM Na_2CO_3-solution with a flow rate of 0.8 mL/min. MRM-suppressor was regenerated by 100 mM H_2SO_4.

2.5. Data analysis

For kinetic analysis, the pseudo first-order model was employed:

$$k = -\frac{\ln(\frac{c}{c0})}{t*} \quad (1)$$

with k being the pseudo first-order rate constant in min^{-1}, c being the measured concentration of the target substance varying with time and c_0 being the initial concentration. Time was calculated $t^* = t - t_{lag}$, where t_{lag} is the activation time of the catalytic system, which means the catalyst needs time to create this reactive manganese species [1].

2.6. Experimental setup

Experiments were conducted in ultrapure water, and additional experiments were conducted in a wastewater matrix: effluent of the secondary clarification stage of the municipal wastewater treatment plant Aachen-Soers, which was filtered through regenerated cellulose (SPARTAN, 0.2 µm, 30 mm) from Whatman (USA). The average values for COD, TOC, DOC, TN_b and P_{total} for the year 2019, when the water was sampled for the experiments, were 18, 6.9, 6.2, 5.7 and 0.1 mg L^{-1}, respectively. The pH of our water sample was 8.5 ± 0.3. These values are similar to secondary effluent characteristics reported in literature [7], with the pH rather being in the upper range. The initial concentration of the target micropollutant DCF or respectively SMX was 10 mg L^{-1}. This concentration was chosen although it was higher than what is typically present in the environment for TPs to be detected. The ratio between micropollutant and H_2O_2 was in the same order of magnitude as in similar studies [8]. The fluid volume for each

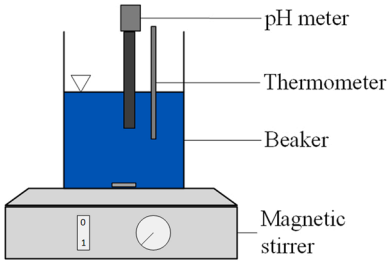

Fig. 3. Experimental setup.

experiment was 30 mL and contained 10 mg L^{-1} TACN-Mn. The solution was constantly stirred in a beaker (see Fig. 3) and pH was kept constant at 8.5 ± 0.5 by adding sodium hydroxide or sulphuric acid. The temperature was kept constant at 20 ± 0.5 °C. After the initial sample was taken, 0.1 mL 30%-H_2O_2 solution was added and another sample was taken. Subsequent samples were taken every 15 min.

As a first approach to improve the TACN-Mn/H_2O_2 system, we examined the combination of TACN-Mn/H_2O_2 with UV. To evaluate the enhanced degradation performance, methylene blue was used as a target substance. As for the experimental procedure, TACN-Mn, and H_2O_2 dosage were the same as in the main experiments for DCF and SMX degradation. The temperature was 20 °C and pH was 7. The setup was irradiated with a UV LED lamp (Fluke, 10 W, 395 nm) from above (not shown).

2.7. Experimental plan

Table 1 gives an overview of the key experiments to demonstrate the efficiency of TACN-Mn/H_2O_2. Reference experiments (only TACN-Mn or only H_2O_2) are included.

This experimental series is based on a preliminary screening (full factorial plan) using 7.4 mg L^{-1} methylene blue to investigate the effect of several parameters in the relevant range: temperature (10 and 20 °C), pH (6 and 9), concentrations of TACN-Mn (10 and 80 mg L^{-1}) and H_2O_2 (1.1 and 10.6 mg L^{-1}). For more information and results see the SI. Since the effect of pH was identified as crucial, additional experiments investigating the effect of pH in the relevant range were conducted.

3. Results and discussion

3.1. Basic reactivity of the TACN-Mn/H_2O_2 system

The basic reactivity of DCF and SMX in the TACN-Mn/H_2O_2 system was investigated with control experiments (only TACN-Mn, only H_2O_2) and in two different water matrices, i.e. ultrapure water and wastewater (Table 1). The results of all eight key experiments are shown in (Fig. 4; Tables 2 and 3).

Degradation experiments were carried out three times, and error bars mark the minimum or maximum normalized concentration. These error bars are only significant during the fast degradation phase where small differences in time make a larger difference in concentration, whereas the differences are negligible at the beginning or end of the experiment. Due to the slower degradation of SMX, the duration of experiments with SMX was prolonged and an additional sample was taken after 240 min.

Table 1
Key experiments for micropollutant degradation.

Exp. No.	Matrix	Micropollutant	H_2O_2	TACN-Mn	Analysis*
1	Ultrapure water	DCF	X	–	DCF, TPs
2	Ultrapure water	DCF	–	X	DCF, TPs
3	Ultrapure water	DCF	X	X	DCF, TPs
4	Treated wastewater	DCF	X	X	DCF, TPs, anions
5	Ultrapure water	SMX	X	–	SMX, TPs
6	Ultrapure water	SMX	–	X	SMX, TPs
7	Ultrapure water	SMX	X	X	SMX, TPs
8	Treated wastewater	SMX	X	X	SMX, TPs, anions

*anions: bromate, chlorite, chlorate
*DCF, SMX degradation and anions (quantitative), TPs (normalized by peak area)

There was no degradation of DCF and SMX with only TACN-Mn or only H_2O_2, but with a combination of them. DCF was degraded almost completely in both matrices as the two very similar curves in Fig. 4 A show. In contrast, the degradation of SMX differed significantly depending on the matrix, and overall, there was less degradation of SMX than of DCF, as seen in Fig. 4 A and C. Competition between degradation of micropollutants and water matrix was larger for SMX than for DCF. From the logarithmic scale displayed in Fig. 4 B and D, the pseudo first-order rate constants can be directly derived (cf. Eq. 1 in Chapter 2.5, using the values of the degradation phase shown in Fig. 4). The corresponding pseudo first-order rate constants are tabulated in Tables 2 and 3, which are discussed in Chapter 3.3.

The concentration of chloride in the ultrapure water tests was 6 mg L^{-1} and in the wastewater tests approx. 200 mg L^{-1} on average. Bromide could only be detected in very small amounts of 0.1 mg L^{-1} in the ultrapure water tests and 0.2 mg L^{-1} in the wastewater experiments. In general, OH radicals, which are the active species in our system, can form further active species with chloride present in water. Depending on the system studied, both an enhancement and a reduction of the degradation rate by inorganic anions was observed [9]. The authors showed that chloride forms ClOH radicals with OH radicals [9]. These radicals are very unstable and decompose back into the chloride ion and the OH radical. The formation rate and decomposition rate are in the same order of magnitude, which means that no great influence can be assumed from these radicals. In the acidic pH range, the formation of Cl radicals was observed, which have a lower reduction potential than OH radicals and could thus adversely affect the degradation rate. The influence of chloride ions on the stability of H_2O_2 could also not be observed in previous studies. The influence of relevant anions (chloride, bromide) in our experiments is estimated to be rather low due to the low measured concentrations and the adjusted alkaline pH. Since anions as well as alkaline conditions cannot be the only reasons for the lower degradation rate of SMX in wastewater, the significantly higher organic load (TOC) of 5.7 mg L^{-1} could be a possible reason. Since OH radicals in the TACN-Mn/H_2O_2 system represent a possible degradation pathway [6,10], they could be involved in nonspecific reactions with organic matter in wastewater. Previous studies with ozone [11] and photocatalysis with TiO_2 [12], both mainly using OH radicals as reactive species, also found the negative influence of organic matter on the degradation rate of SMX. In both studies, a decrease in the degradation rate constant k of SMX was observed from initial values in pure water (ozone: 2.9×10^{-3} s^{-1}; photocatalysis: 5.44×10^{-1} min^{-1}; TACN-Mn/H_2O_2: 1.86×10^{-2} min^{-1}) to lower values after the addition of organic matrix components (ozone: 0.9×10^{-3} s^{-1} (5 mg L^{-1} Humic substances); photocatalysis: 1.41×10^{-1} min^{-1} (5 mg L^{-1} Suwannee River NOM) (5 mg L^{-1}); TACN-Mn/H_2O_2: 5.84×10^{-3} min^{-1} (5.7 mg L^{-1} TOC)). We suppose that the reactive species (OH radicals) are scavenged by the organic matter which competes with SMX for the OH radicals. Thus, the resulting available OH radical concentration is lowered which decreases the degradation rate constant. The presence of organic matter also reduced the degradation rate constant of DCF by 42% (TACN-Mn/H_2O_2: 1.20×10^{-1} min^{-1} without wastewater matrix; 6.96×10^{-2} min^{-1} with wastewater matrix). In previous studies, different observations of the influence of organic matter on the degradation rate constant of DCF could be made. The use of ionizing radiation based on OH radicals also demonstrated a reduction of up to 71% in the degradation rate of DCF at high organic matter levels 30–80 mg L^{-1} [13]. Apparently, DCF decomposes more easily than SMX, which is why the reaction time was extended. If organic matter in the wastewater reduces the concentration of the active species, this is no longer sufficient to degrade SMX, but it is still sufficient to degrade DCF.

3.2. Increased reaction kinetics and accelerated catalyst activation at elevated pH

Results of additional experiments investigating the effect of pH in the

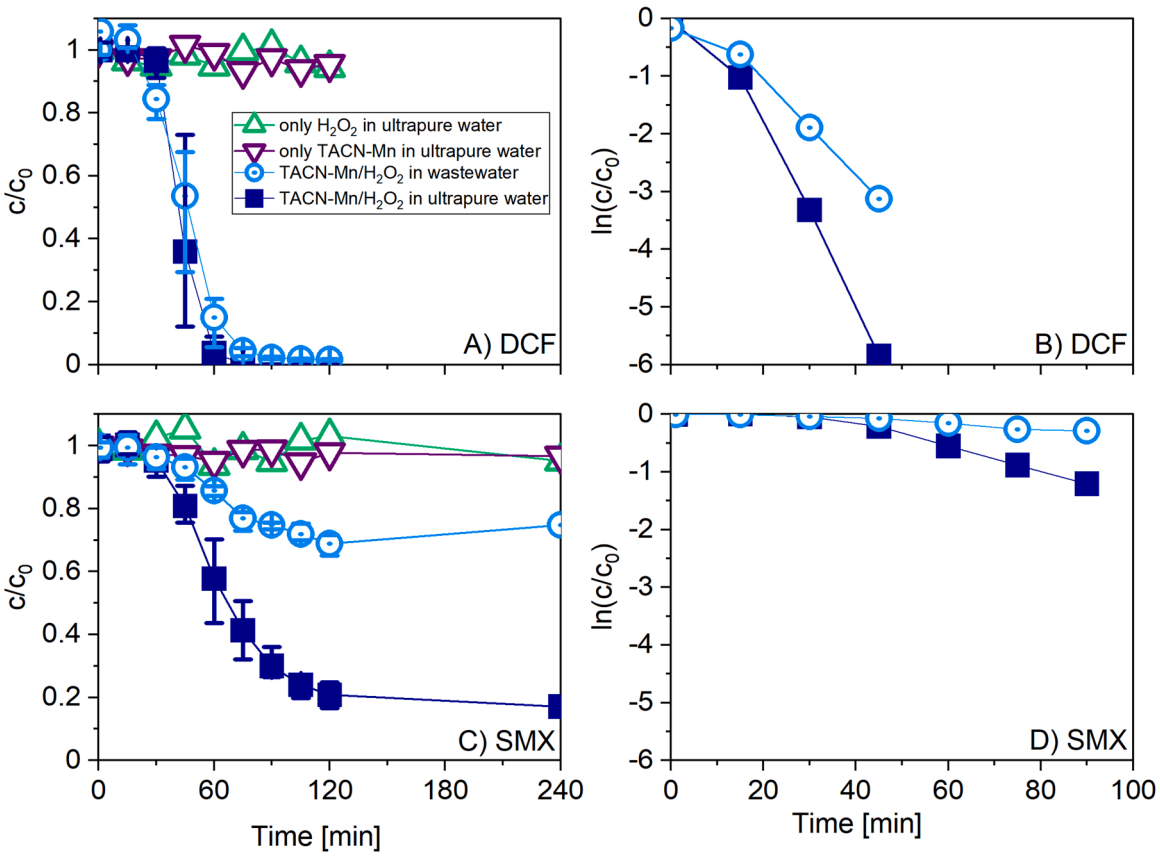

Fig. 4. Degradation of DCF (A, B) and SMX (C, D) in two different water matrices (ultrapure water and treated municipal effluent). pH = 8.5 and T = 20 °C. Initial concentration of DCF and SMX: 10 mg L^{-1}. 10 mg L^{-1} TACN-Mn and H_2O_2 dosage as indicated. Experiments 1–4 from Table 1 are shown in A and B and experiments 5–8 in C and D.

relevant range are shown in Fig. 5.

Fig. 5A shows that degradation rates are strongly dependent on the pH in the investigated range for DCF: the higher the pH, the higher is the degradation. For SMX the pH dependence is less distinct. Due to the selected pH range of 7.5–9, both DCF ($pK_a = 4.2$) and SMX ($pK_1 = 1.97$ and $pK_2 = 6.16$) can be assumed to be present in their ionic species [14, 15].

In our study, SMX showed a significantly lower degradation rate compared to DCF, like in previous studies [16]. In previous studies, this difference was attributed to the formation of reactive transformation products that react with ozone. Since ozone and the TACN-Mn system are both based on OH radicals as reactive species, this explanation could also apply to the TACN-Mn system. A flattening in the degradation curve of SMX can be seen in our experiments as well as in previous studies [16, 17]. It could be shown in previous studies that SMX in both its neutral and its anionic form (pH: 3–8) exhibited the same reactivity and degradation rate towards OH radicals [16,17]. The result of both previous observations given above is a possible explanation for the similar or slightly poorer degradation rate of SMX regardless of pH in the higher alkaline range (pH: 8–9). DCF in its anionic form exhibits higher reactivity with OH radicals. The higher activity is partly due to the stronger hydrogen bonding between the oxygen atom of the carboxy group and the amine hydrogen [18]. In contrast, the neutral form of DCF has a higher activation barrier and is, thus, slightly thermodynamically and kinetically disadvantaged. Beside the high influence on the present species of SMX and DCF, pH also has an effect on the TACN-Mn/H_2O_2 system. Previous studies with dye bleaching [19] have shown that the bleaching and oxidation effect of the catalytic system we used increases up to a pH of 11 (with a maximum at 11) and then decreases, which is why optimization of the conditions for use in real wastewater was carried out. One reason for the drop from a pH of 11 is the decomposition of the catalyst to manganese dioxides and also the degradation of the 1,4,7-trimethyl-1,4,7-triazacyclononane (Me_3TACN) ligands [19]. Due to the delay in the reaction time (lag time) caused by the formation of different manganese species in our experiments, it can be assumed that even at the pH range of 7.5–9 used by us, both mono- and dinuclear manganese species are present, which are both able to form active species. In addition to the pH dependence of the TACN-Mn/H_2O_2 system, it was shown that the formation of OH radicals is preferred in alkaline conditions since the amount of the main precursor hydroxyl anion (OH^-) present is higher under alkaline conditions [20].

3.3. Discussion of reaction kinetics and comparison with Fe-based catalysts

As mentioned before, the TACN-Mn/H_2O_2 system possesses characteristic kinetics: It has a certain activation time (cf. Chapter 2.5). This activation time varied widely for both DCF and SMX depending on the pH (cf. Chapter 3.2). The pseudo first-order rate constants of this study were calculated according to Eq. 1 in Chapter 2.5 and are presented in Table 2 for DCF (1.06×10^{-1} to 4.45×10^{-3} min^{-1}) and in Table 3 for SMX (2.33×10^{-2} to 1.62×10^{-3} min^{-1}). These calculated rates quantify and confirm our previous qualitative observations (cf. Chapter 3.2), that SMX showed a significantly lower degradation rate compared to DCF. The effect of the pH value is also quantified. When the pH is decreased from 9 to 7.5, the rate constant for DCF decreases from 1.06×10^{-1} to 4.45×10^{-3} min^{-1} and for SMX from 1.72×10^{-2} to 1.62×10^{-3} min^{-1}. A clear slowdown is evidenced by the above-mentioned figures. When wastewater is used, the rate constant decreases to 6.96×10^{-2} min^{-1} for DCF and 5.84×10^{-3} min^{-1} for SMX. This again indicates that due to the

Table 2
Kinetic rate constants from literature for the degradation of DCF.

System	DCF conc. [g L^{-1}]	Water matrix	Experimental conditions	k [min^{-1}]	Reference
			pH = 7.5; T = 20 °C	4.45×10^{-3}	
			pH = 8; T = 20 °C	3.15×10^{-2}	
			pH = 8.5; T = 20 °C	1.20×10^{-1}	
		Ultrapure water	pH = 9; T = 20 °C	1.06×10^{-1}	
TACN-Mn/H_2O_2	1.00×10^{-2}	Treated municipal effluent	pH = 8.5; T = 20 °C	6.96×10^{-2}	this study
Fe(II)-activated peracetic acid	2.96×10^{-4}	Ultrapure water	pH = 6–7; T = 25 °C	1.10×10^{1}	[27]
UV/selenium nanoparticles/H_2O_2	4.00×10^{-2}	Ultrapure water	pH = 7,5	7.38×10^{-2}	[22]
Potassium permanganate	5.00×10^{-5}	Ultrapure water; wastewater effluent; surface water	pH = 7; T = 20 °C	3.51×10^{-6} to 9.62×10^{-6}	[28]
Hydroxyl radical and hydrated electron	5.45×10^{-2}	Phosphate buffer	pH = 7; T = 25 °C	9.84×10^{7} to 5.24×10^{8}	[23]
Pyrite Fenton	5.03×10^{-3}	Ultrapure water	pH = 4; T = 25 °C	9.84	[24]
UV/TiO_2	5.00×10^{-3} to 2.00×10^{-2}	Deionized water; groundwater; treated municipal effluent	pH = 6; T = 23 °C	1×10^{-2} to 3×10^{-2}	[21]
Ozone	8.00×10^{-3}	Ultrapure water	pH = 7; T = 20 °C	1.06×10^{3}	[29]
UV/H_2O_2 and ozone	8.88×10^{-2}	Ultrapure water	pH = 5–6; T = 25 °C	3.17×10^{2}	[30]

Table 3
Kinetic rate constants from literature for the degradation of SMX.

System	SMX conc. [g L^{-1}]	Water matrix	Experimental conditions	k [min^{-1}]	Reference
			pH = 7.5; T = 20 °C	1.62×10^{-3}	
			pH = 8; T = 20 °C	2.33×10^{-2}	
			pH = 8.5; T = 20 °C	1.86×10^{-2}	
		Ultrapure water	pH = 9; T = 20 °C	1.72×10^{-2}	
TACN-Mn/H_2O_2	1.00×10^{-2}	Treated municipal effluent	pH = 8.5; T = 20 °C	5.84×10^{-3}	this study
UV/ peroxymonosulfate	1.00×10^{-3}	Pure water	pH = 3.7; T = 25 °C	3.60×10^{-1}	[31]
mZVI/H_2O_2	6.33×10^{-3}	Pure water	pH = 3; T = 20 °C	4.00×10^{-2} to 1.40	[32]
Ultrasound/ozone	1.00×10^{-1}	Pure water	pH= 7	7.13×10^{-1}	[33]
CoFe/AgFe/ persulfate	1×10^{-2}	Deionized water	pH= 5.67	4.8×10^{-2} to 9.9×10^{-2}	[34]
Potassium permanganate	5.00×10^{-3}	Pure water	pH = 7; T = 20 °C	7.13×10^{-2}	[35]
Microwave/ persulfate	1.26×10^{-2}	Deionized water	pH = 4.7; T = 60 °C	2.59×10^{-2}	[36]
Solar photo-Fenton	5.00×10^{-2}	Distilled water; seawater	pH = 2.5–2.8; T = 25 °C	1.00×10^{-1}	[37]
Ozonation	1.26×10^{-1}	Buffer solution	pH = 5; T = 20 °C	2.88×10^{-1}	[38]

different structural properties of the molecules, a smaller amount of active species suffices for the degradation of DCF than for SMX.

We compared our results to various experiments reported in literature, investigating the same substances in similar experimental designs. As Table 2 for DCF and in Table 3 for SMX show, our results compare well to the results of other AOP studies. For example, in one study the same initial concentration of DCF was used and very similar pseudo first-order rate constants (1×10^{-2} to 3×10^{-2} min^{-1}) were found although a different catalytic system with UV activation was used [21]. Not only a catalyst and UV irradiation, but also H_2O_2 was used in another study, leading to a slightly higher rate constant (7.38×10^{-2} min^{-1}) at the pH of 7.5 than in our study (4.45×10^{-3} min^{-1}) [22]. Some studies reached significantly higher rate constants (9.84×10^{7} to 5.24×10^{8} min^{-1}), using different technologies like pulse radiolysis and ϒ irradiation [23]. Consistent with our findings, degradation rate constants for SMX are lower than for DCF in all investigated studies (cf. Table 2 and Table 3).

For the comparison between TACN-Mn/H_2O_2 and other systems, studies of Fe-based catalysts are of special interest [24] because they are considered the benchmark process for H_2O_2 catalysis. Hence such studies are numerous and constantly being developed to increase catalytic activity and, thus, increase reaction kinetics [25]. For example, Fe-based nanoparticles were integrated in a carbon matrix and the enhanced performance was attributed to the high surface area and possible synergistic effects of the components [26]. In contrast to TACN-Mn, conventional Fe-based catalysts usually work best at an acidic pH of about 3, which is far outside the pH range of municipal wastewater. To overcome this major drawback, chelating agents are used and thus the working pH range enlarges up to neutral pH. The use of chelating agents, however, increases TOC and operating cost and, therefore, should be kept to a minimum. TACN-Mn, on the other hand works in the neutral to alkaline pH range of municipal wastewater without any additional chemicals.

3.4. Identification of transformation products and transformation pathways

For most of the TPs formed by DCF and SMX, no commercially obtainable standards are available for identification. To allow comparison between the TPs, the peak area ratio of M-H and M+H was taken and normalized to 1 for the highest peak area intensity of all samples. In many cases, multiple isomers could be observed, and here no individual isomers were identified. An example of this is the mono hydroxylated TP 311, for which several isomers were seen in the chromatogram of the LC measurement. In general, the isomer with the highest area intensity was used for illustration. Possible TPs were described according to their nominal mass. An overview of possible degradation products of DCF and SMX obtained by LC-HRMS can be found in Table 1 and Table 2 in the SI. The main degradation pathways and the corresponding TPs were additionally framed. Since analysis by IC revealed no evidence of bromate, chlorite, or chlorate formation, discussion of inorganic TPs was not included in this study.

Through LC-HRMS analysis, nine major TPs were identified and are

shown in Fig. 6. The literature research showed that the degradation of DCF often occurs through OH radicals, mainly through the hydroxylation of the aromatic rings, the cleavage of the -COOH group, or Cl atoms of DCF as well as the amino group [22,39–44]. From DCF, TP 311 was identified with an accurate mass of 311.0109 and an elemental composition of $C_{14}H_{11}Cl_2NO_3$. In addition, peaks at 12.22 and 10.75 min were found for the extracted ion chromatogram (EIC). TP 311 (three isomers) is a well-known TP of OH radical-based reactions and is formed by hydroxylation on the aromatic rings of DCF. In past studies, three isomers with an exact mass of 311.0114 (TP 311) could be identified [23]. A formation of constitutional isomers could, therefore, be the cause for the different peaks for the same EIC. In the case of TPs 311-a and -b, this is phenylacetic acid ring, in TP 311-c that of 2,6-dichloroaniline [45]. Even though OH radicals act as non-specific electrophilic oxidants, it is nevertheless assumed that position 5 in the para position to the NH substituent is preferentially attacked at the more electron-rich aromatic ring. The di-hydroxylated DCF (TP 327) was also identified with an exact mass of 324.9909 and elemental composition $C_{14}H_9Cl_2NO_4$. It has been suggested that the additional hydroxyl group is attached to the non-hydroxylated ring [23,46]. Another peak with an exact mass of 308.9959 and elemental composition of $C_{14}H_9Cl_2NO_3$ indicated a similar molecular structure as TP 311. Further oxidation of TP 311-a of the mono-hydroxylated DCF leads to a quinone-imine intermediate. The hydroxylated quinone-imine product TP 324 was also identified with an exact mass of 327.0065 and an elemental composition of $C_{14}H_{11}Cl_2NO_4$. In past studies, these species were also detected and considered as evidence for degradation by OH radicals [43,47,48]. TP 161 could be identified as 2,6-dichloroaniline with a retention time of 7.5 min and an exact mass of 160.9799 and the elemental composition $C_6H_5Cl_2N$ [27,39,45]. A similar degradation pathway is the formation of TP 151 (5-hydroxy-phenylacetic acid), which also forms when the CN bond is cleaved by OH radicals, where the amino group, however, remains on the ring of 1,4-dichloroanniline. TP 151 (5-amino-phenylacetic acid) was also observed as an alternative degradation pathway [30,46]. In this degradation mechanism, the amino group remains on the phenylacetic acid substituent. Another degradation mechanism occurs via the breakdown of the carboxy group of DCF. The decarboxylation of DCF leads to TP 251, which was identified as 2, 6-dichloro-N-(o-tolyl)aniline with an exact mass of 251.0266 and elemental composition $C_{13}H_{11}Cl_2N$. One peak at 12.78 and an exact mass of 265.0061 and the elemental composition $C_{13}H_9Cl_2NO$ could be identified as 2-(2,6-dichlorophenylamino)benzaldehyde. Another peak TP 267 at 13.44 min and an exact mass 267.0211 and elemental composition $C_{13}H_{11}Cl_2NO$ revealed the formation of {2-[(2,6-dichlorophenyl)amino]phenyl}methanol. Both TPs are formed by decarboxylation (TP 251) and subsequent hydroxylation to TP 267 and further oxidation of the alcohol group to aldehyde TP 265. Similar degradation pathways could also be observed in processes with UV/peracetic acid [49], boron-doped diamond electrodes [41], photocatalysis [39], and photo-Fenton systems [43]. Starting from TP 265, TP 281 could also be identified with an exact mass of 281.0010 and represents the mono hydroxylated TP 265.

Fig. 7 shows the time-dependent degradation profiles of DCF in TACN-Mn/H_2O_2 at pH 8.5 in ultrapure water and effluent wastewater. The plot of the area ratio (Fig. 7) at the beginning (t = 0 min) and at the respective sampling intervals shows that the majority of the TPs reach their maximum at the end of the reaction period between 60 and 120 min with a time delay for the formation of the catalytic system of about 50 min. TP 251, on the other hand, decreases again after 60 min reaction time, which could happen because the methyl group is oxidized to the corresponding alcohol or aldehyde group. TP 151b (5-amino-phenylacetic acid) also decreases after 60 min. A comparison of the relative degradation in ultrapure water and wastewater shows that the TPs in wastewater exhibit a lag time similar to the degradation of the

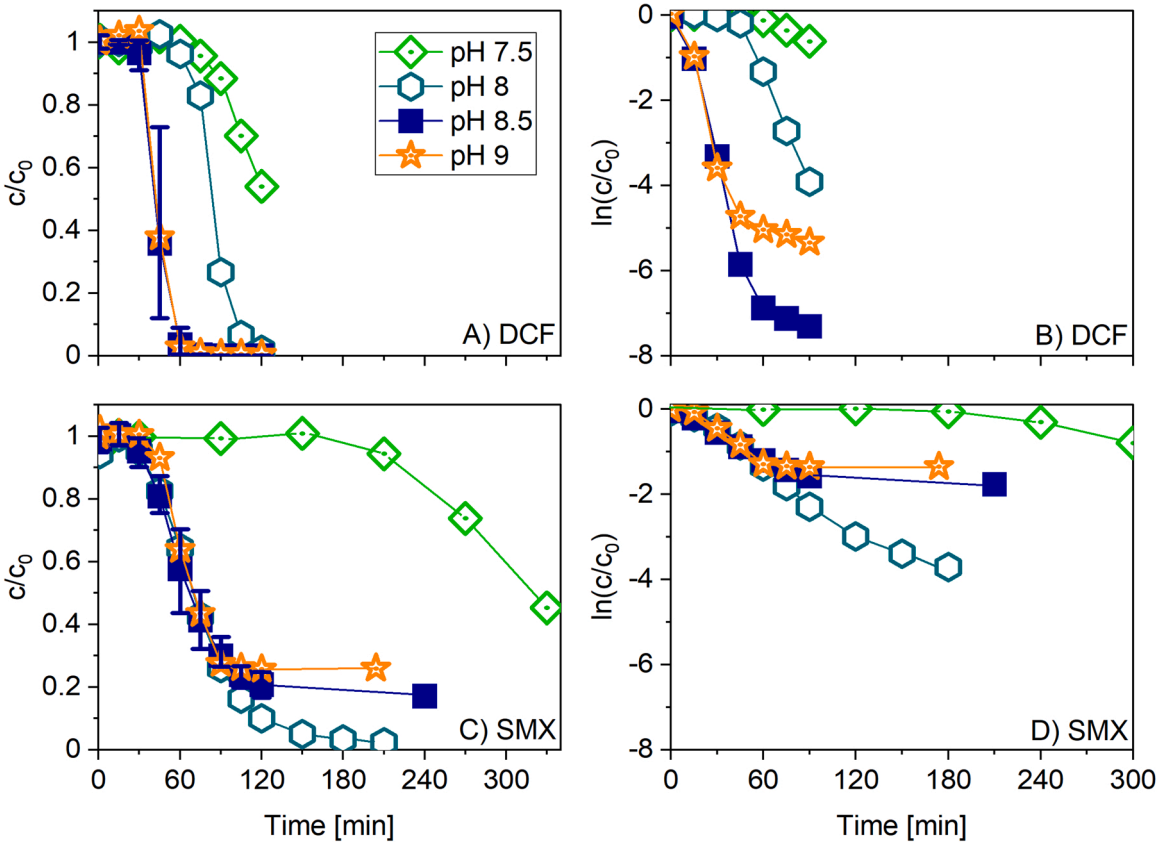

Fig. 5. Degradation of DCF (A and B) and SMX (C and D) in ultrapure water at different pH values: pH 7.5, 8, 8.5 and 9. T = 20 °C, 10 mg L^{-1} TACN-Mn and H_2O_2 dosage as indicated. Initial concentration of DCF and SMX: 10 mg L^{-1}.

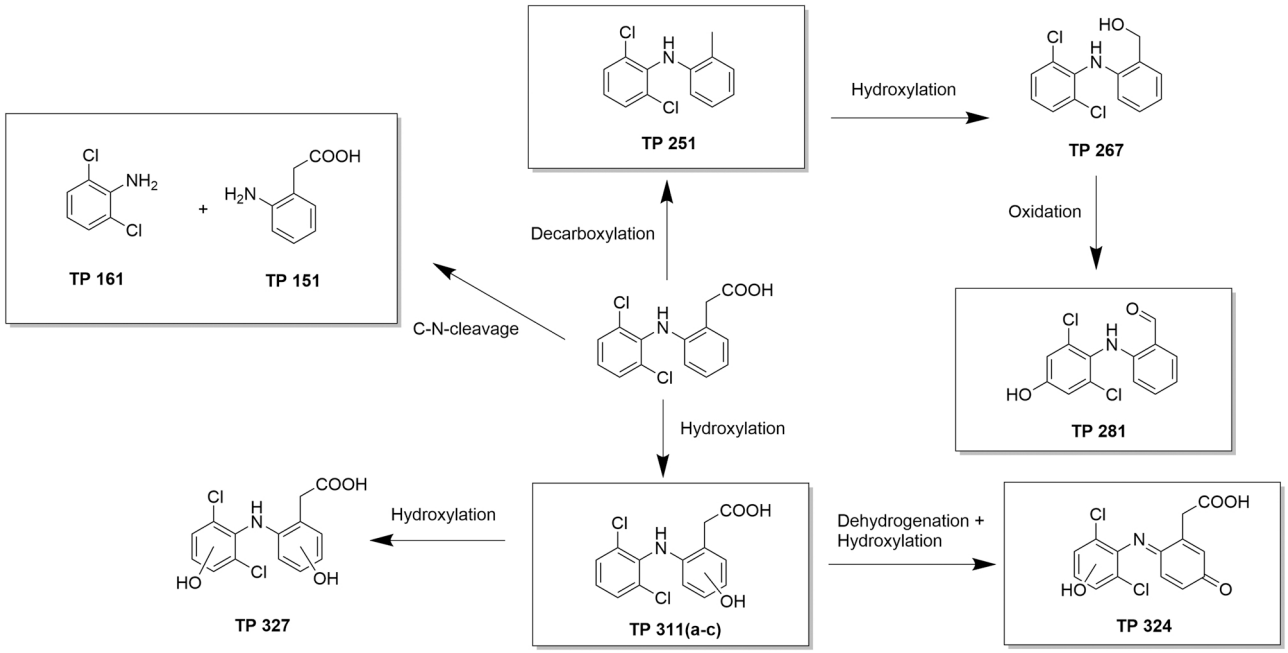

Fig. 6. DCF degradation pathways in TACN-Mn/H_2O_2 process.

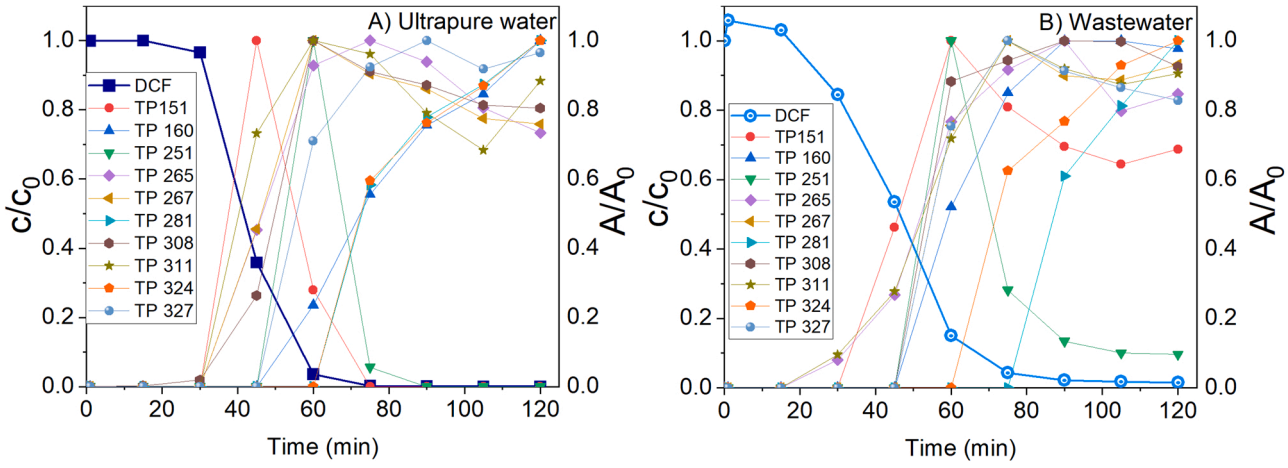

Fig. 7. Time-dependent profiles of major degradation products of DCF (A/A_0) in TACN-Mn/H_2O_2 process at pH 8.5 in wastewater and ultrapure water.

parent substance. The delay could be due to matrix effects, such as secondary reactions of the active species. It was proposed that the further degradation of the resulting transformation products from the cleavage of the C-N bond leads to mineralization in which inorganic degradation products HCl and CO_2 are formed [50]. Since only transformation products were investigated by LC-HRMS (cut-off <40 *m/z*), no conclusions can be drawn about the formation of low molecular weight compounds such as CO_2.

Through LC-HRMS analysis, seven major TPs of SMX were identified and are shown in Table 2 in the SI. The literature research showed that the degradation of SMX occurs through OH radicals, mainly through the hydroxylation of the aromatic rings, the cleavage or oxidation of the amino group (-NH_2), and the cleavage of the S-N bond. TP269 with the exact mass of 269.0470 shows the addition of an oxygen atom. In other AOP processes, based on OH radicals, an attack on the aromatic ring of the aniline structure is assumed [33,35,51,52]. An analysis of the fragment spectrum cannot show a difference in oxygen atom binding to either the amino group or the aromatic ring of the aniline. It is assumed that an electrophilic addition preferentially takes place at the aromatic ring in the ortho-position [32]. It could be shown that the anionic species of SMX are preferentially attacked at the amide nitrogen, while one of the aromatic rings is preferred for the neutral species of SMX [53]. It is suggested that OH radicals attack the neutral species non-selectively, while for the anionic species the oxazole ring could be preferentially attacked by the deprotonated amide nitrogen due to the higher electron density [52,54]. It has been shown that for this reason higher pH values promote the degradation performance of SMX during ozonation and oxidation with $KMnO_4$ [54]. Differentiation of the TP at different pH values was not carried out in our study, since the TACN-Mn as a bleach catalyst reacts preferentially only in the alkaline environment. Based on the experiments and the set pH values of 7–9, both the neutral and the anionic variants of SMX are present. TP 238 with the exact mass 238.0412 and TP 254 result from the cleavage of the amino group (oxidative deamination) and hydroxylation of the aromatic ring. These TPs were also postulated by [55,56]. The attack of an OH radical on the sulfonamide bond leads to cleavage of the SMX and results in TP 98. The counterpart would be 4-aminobenzo sulfonic acid. This TP could not be observed in this study. Instead, TP 139 could be detected as

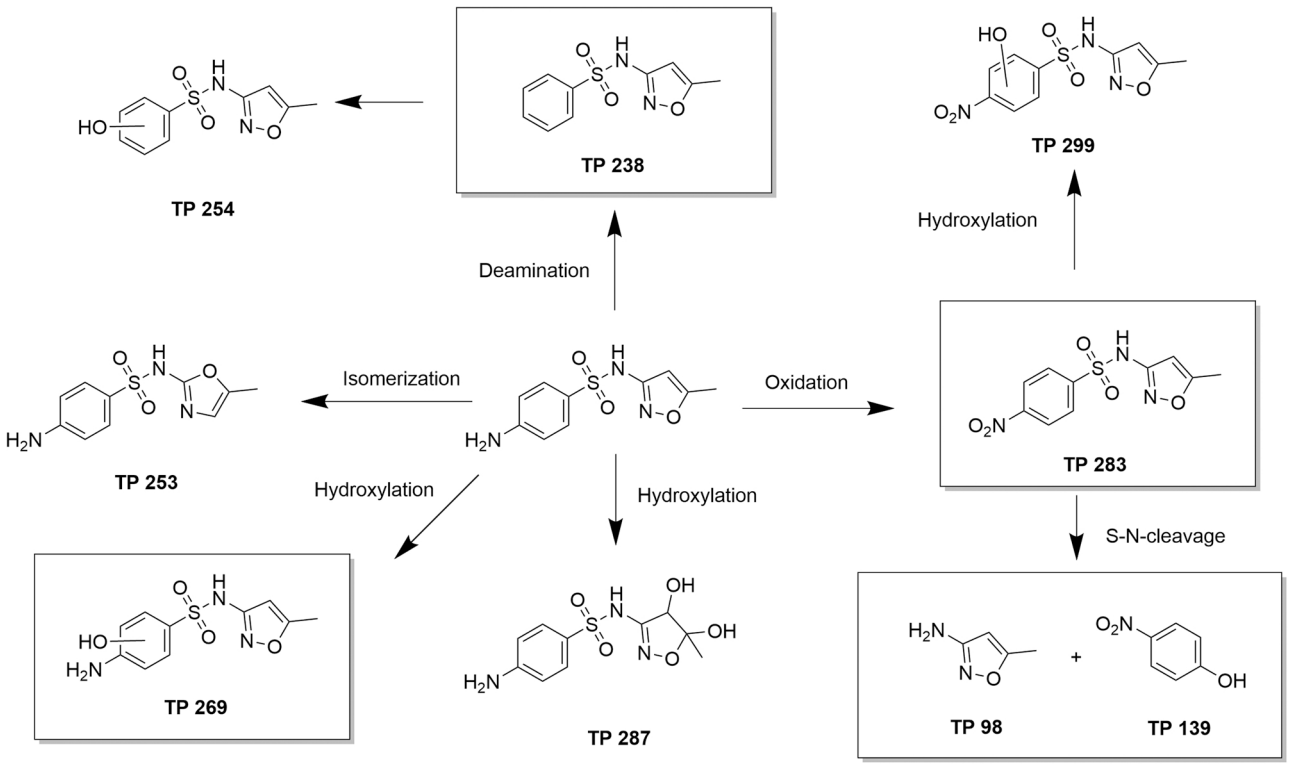

Fig. 8. SMX degradation pathways in TACN-Mn/H_2O_2 process.

4-nitrophenol, which indicates that sulfate is cleaved off during bond breakage, followed by hydroxylation in the para position of the oxidized amino group. The oxidation of the amino group of the aniline ring to the nitro group leads to the formation of TP 283 with an exact mass of 283.0263 and could be identified as nitro-SMX. Another degradation pathway is the attack of an OH radical on the electron-rich double bond of the isoxazole ring, leading to TP 287 with the exact mass of 286.0497 [57]. Another transformation is TP 253, which is an isomer of SMX and could be detected by photocatalytic methods. Compared to SMX, it elutes 2 min earlier and has the same exact mass of 253.0521. TP 253 is an isomer of SMX, which is mainly formed by photo-isomerization [56, 58].

Fig. 9 shows the time-dependent degradation profiles of SMX in TACN-Mn/H_2O_2 at pH 8.5 in ultrapure water and effluent wastewater. In comparison to DCF, a longer lag time can be seen before the degradation of SMX begins. In contrast to the TPs of SMX, no further degradation of the TPs is evident here. The majority of the TPs are formed with $A/A_0 > 50$ after 100 min

The majority of DCF is degraded or converted to more highly oxidized TPs, which could have higher toxicity than the parent substance. Thus, they can also serve as precursors for toxic disinfection by-products such as halobenzoquinones [59]. Chlorination of paracetamol showed that quinone-imine intermediates cause liver necrosis and are, thus, more toxic than the parent compound [60]. In addition, they decompose in aqueous conditions to the toxic 1,4-benzoquinone, which, due to its structural similarity, could also contribute to renal toxicity [61]. Photo-TPs of DCF could show a six-fold increase of phytotoxicity in algal reproduction compared to the parent compounds [62]. It has been shown that the synergistic effects of the nitrogenous TPs can contribute to the overall toxicity [63]. Most of the SMX is degraded or transformed to higher oxidized TPs, which might have higher toxicity than the parent substance. In studies where the parent compound and TPs of SMX were

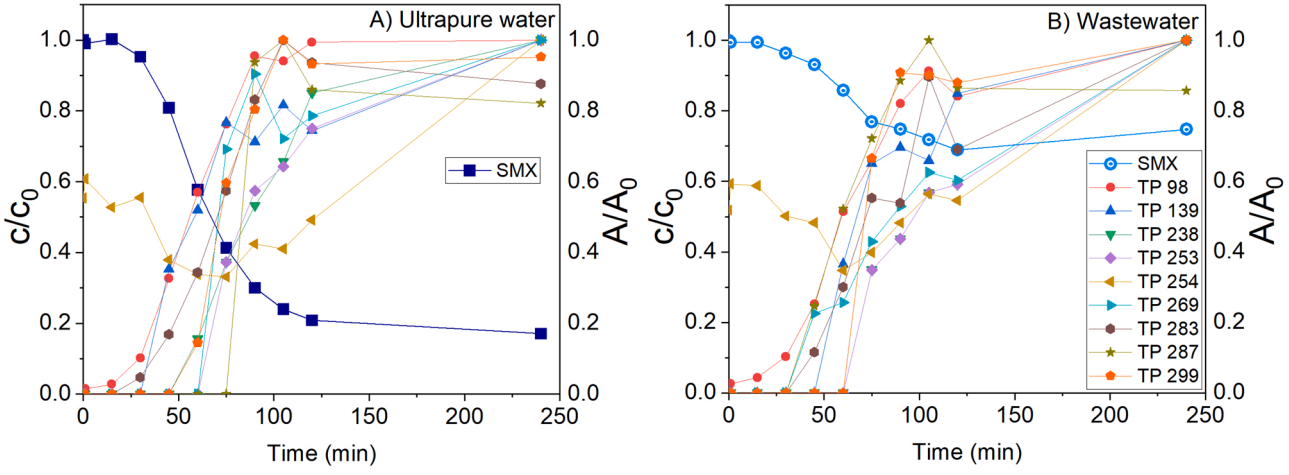

Fig. 9. Time-dependent profiles of major degradation products of SMX in TACN-Mn/H_2O_2 process at pH 8.5 in wastewater and ultrapure water.

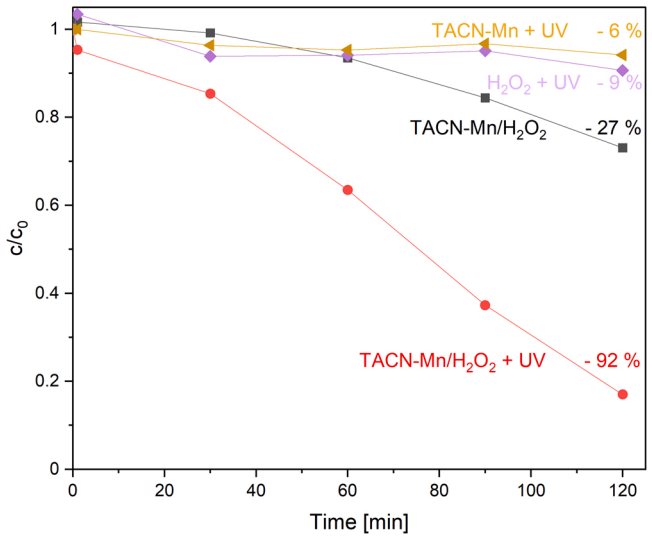

Fig. 10. Combination of TACN-Mn/H_2O_2 with UV (10 W, 395 nm) for methylene blue degradation. T = 20 °C, pH = 7 and c_0 = 7.4 mg L^{-1}.

estimated by ECOSAR, aquatic toxicity was shown to decrease after the degradation of SMX and the formation of TPs [64]. The mixture toxicity of DCF and SMX with their TPs is largely unexplored and unknown, and would need further research.

3.5. *Enhancement of TACN-Mn/H_2O_2-system and prospects for technical application*

As Fig. 10 shows, UV light accelerated activation and kinetics of the TACN-Mn/H_2O_2 system so that degradation increased from 27 % to 92 %. The effects of the three components individually (TACN-Mn or H_2O_2 or UV) were all negligible (not shown) as well as the effect of UV on the single components TACN-Mn or H_2O_2 (shown in Fig. 10). This first approach to improve the performance of the catalytic system is promising and needs to be investigated further to gain a good understanding of possible synergy effects.

For a successful implementation of the TACN-Mn/H_2O_2-system on wastewater treatment plants, several additional challenges have to be addressed in future research: Separation of TACN-Mn from the treated wastewater stream and subsequent recirculation have to be investigated. A membrane filtration step is most likely required to ensure sufficient retention. According to the molecular size of TACN-Mn (129 + 55 g mol^{-1}), tight nanofiltration membranes with a molecular weight cut-off in the lower range could be considered. Resulting from the prior advanced wastewater treatment, foulants may be already reduced to a large extent. However, it must be ensured that the membrane is not affected negatively by H_2O_2. Furthermore, possibilities to immobilize TACN-Mn should be examined because this immobilization would facilitate the separation step. One possibility to inactivate TACN-Mn after the oxidation process would be to use polymer-bound TACN derivatives, which could be removed by membrane filtration since they have higher molecular weight [65]. In past studies it could already be shown that the polymerized TACN derivatives exhibit similar catalytic activity as their monomeric systems [66].

Furthermore, when the ligands are modified to increase the catalytic activity, the catalyst can be improved, which could e.g. shorten the lag time for the formation of the active species [5].

4. Conclusions

TACN-Mn was demonstrated to be an effective catalyst for AOPs in ultrapure water and wastewater treatment plant effluent. The key influencing factor of the catalytic reaction was shown to be its pH dependency. The ideal pH in the investigated range is above 8, but micropollutant abatement was also observed at lower pH values. In wastewater, the oxidation is still effective, but at a lower rate and to a lesser extent as compared to ultrapure water. TPs and reaction pathways/mechanisms for DCF and SMX were elucidated by LC-HRMS. Such transformations, which only change the structures of DCF to a minor degree, can also pose environmental risks in wastewater. For future investigations the two following aspects have to be pursued: Firstly, the TPs need to be characterized more closely to evaluate their toxicity. For exact accounting of TPs, experiments with radiolabelled micropollutants could be conducted. Secondly, the TACN-Mn/H_2O_2-AOP system must be optimized further from the process engineering point of view, and the potential of TACN-Mn immobilization needs to be used for effective separation.

Funding

This work was supported by the Federal Ministry of Education and Research of Germany (BMBF) [project PEPcat, grant number 02WCL1519A] and the European Regional Development Fund (EFRE 2014–2020) [project µ3 - Forschungszentrum Soers - Emerging Pollutants Research Center Aachen, grant number EFRE 0500123 / 1809FI03].

CRediT authorship contribution statement

Julia Wolters: Conceptualization, Methodology, Validation, Formal analysis, Investigation, Writing – original draft, Visualization, Project administration, **Muhammad Usman:** Conceptualization, Methodology, Validation, Formal analysis, Investigation, Writing – original draft, Visualization, **Johanna Mathiä:** Investigation, **Dirk Dirichs:** Investigation, **Daniel Bastian:** Conceptualization, Funding acquisition, **Benedikt Aumeier:** Writing – Reviewing and editing, **Carsten Bolm:** Writing – review & editing, Supervision. **Volker Linnemann:** Writing – review & editing, Supervision, Funding acquisition. **Thomas Wintgens:** Writing – review & editing, Supervision, Funding acquisition.

Declaration of Competing Interest

The authors declare that they have no known competing financial interests or personal relationships that could have appeared to influence the work reported in this paper.

Data Availability

Data will be made available on request.

Acknowledgments

The authors would like to thank Ronald Hage and CATEXEL for providing the catalyst, the laboratory staff and student assistants of ISA, RWTH Aachen University for their assistance. We would like to especially acknowledge Dr. Nico Meyer (deceased) for his enthusiastic support and tremendous spirit.

Appendix A. Supporting information

Supplementary data associated with this article can be found in the online version at doi:10.1016/j.jece.2022.108320.

References

[1] J.R. Lindsay Smith, B.C. Gilbert, A. Mairata i Payeras, J. Murray, T.R. Lowdon, J. Oakes, R. Pons i Prats, P.H. Walton, Manganese 1,4,7-trimethyl-1,4,7-triazacyclononane complexes: versatile catalysts for the oxidation of organic compounds with hydrogen peroxide, J. Mol. Catal. A: Chem. 251 (2006) 114–122, https://doi.org/10.1016/j.molcata.2006.02.025.

[2] R. Hage, J.W. de Boer, F. Gaulard, K. Maaijen, Manganese and iron bleaching and oxidation catalysts, in: Advances in Inorganic Chemistry, Academic Press Inc, 2013, pp. 85–116, https://doi.org/10.1016/B978-0-12-404582-8.00003-1.

[3] B.C. Gilbert, J.R. Lindsay Smith, A. Mairata, I. Payeras, J. Oakes, R. Pons, I. Prats, A mechanistic study of the epoxidation of cinnamic acid by hydrogen peroxide catalysed by manganese l,4,7-trimethyl-l,4,7-triazacyclononane complexes, J. Mol. Catal. A: Chem. 219 (2004) 265–272, https://doi.org/10.1016/j.molcata.2004.05.012.

[4] B.C. Gilbert, J.R.L. Smith, A. Mairata I Payeras, J. Oakes, Formation and reaction of O=MnV species in the oxidation of phenolic substrates with H_2O_2 catalysed by the dinuclear manganese(IV) 1,4,7-trimethyl-1,4,7-triazacyclononane complex [Mn IV2(μ-O)3(TMTACN)2](PF 6)2, Org. Biomol. Chem. 2 (2004) 1176–1180, https://doi.org/10.1039/b315427k.

[5] R. Hage, J.E. Iburg, J. Kerschner, J.H. Koek, E.L.M. Lempers, R.J. Martens, U. S. Racherla, S.W. Russell, T. Swarthoff, M.R.P. van Vliet, J.B. Warnaar, L. van der Wolf, B. Krijnen, Efficient manganese catalysts for low-temperature bleaching, Nature 369 (1994) 637–639, https://doi.org/10.1038/369637A0.

[6] R. Hage, A. Lienke, Applications of transition-metal catalysts to textile and wood-pulp bleaching, Angew. Chem. - Int. Ed. 45 (2005) 206–222, https://doi.org/10.1002/ANIE.200500525.

[7] M. Villanueva-Rodríguez, R. Bello-Mendoza, A. Hernández-Ramírez, E.J. Ruiz-Ruiz, Degradation of anti-inflammatory drugs in municipal wastewater by heterogeneous photocatalysis and electro-Fenton process, Environ. Technol. 40 (2019) 2436–2445, https://doi.org/10.1080/09593330.2018.1442880.

[8] A. Ameri, M. Shakibaie, M. Pournamdari, A. Ameri, A. Foroutanfar, M. Doostmohammadi, H. Forootanfar, Degradation of diclofenac sodium using UV/biogenic selenium nanoparticles/H_2O_2: optimization of process parameters, J. Photochem. Photobiol. A: Chem. 392 (2020), https://doi.org/10.1016/j.jphotochem.2020.112382.

[9] J. Wang, S. Wang, Effect of inorganic anions on the performance of advanced oxidation processes for degradation of organic contaminants, Chem. Eng. J. 411 (2021), 128392, https://doi.org/10.1016/J.CEJ.2020.128392.

[10] J.M. Gould, Studies on the mechanism of alkaline peroxide delignification of agricultural residues, Biotechnol. Bioeng. 27 (1985) 225–231, https://doi.org/10.1002/BIT.260270303.

[11] X. Liu, T. Garoma, Z. Chen, L. Wang, Y. Wu, SMX degradation by ozonation and UV radiation: a kinetic study, Chemosphere 87 (2012) 1134–1140, https://doi.org/10.1016/J.CHEMOSPHERE.2012.02.007.

[12] R. Yuan, Y. Zhu, B. Zhou, J. Hu, Photocatalytic oxidation of sulfamethoxazole in the presence of TiO2: Effect of matrix in aqueous solution on decomposition mechanisms, Chem. Eng. J. 359 (2019) 1527–1536, https://doi.org/10.1016/J.CEJ.2018.11.019.

[13] R. Zhuan, J. Wang, Degradation of diclofenac in aqueous solution by ionizing radiation in the presence of humic acid, Sep. Purif. Technol. 234 (2020), 116079, https://doi.org/10.1016/J.SEPPUR.2019.116079.

[14] L. Zheng, H. Jin, M. Yu, Q. Zhongwei, L. Zhang, C. Shikun, Z. Li, Degradation of sulfamethoxazole by electrochemically activated persulfate using iron anode, Int. J. Chem. React. Eng. 17 (2019), https://doi.org/10.1515/ijcre-2018-0160.

[15] H. Cheng, D. Song, H. Liu, J. Qu, Permanganate oxidation of diclofenac: the pH-dependent reaction kinetics and a ring-opening mechanism, Chemosphere 136 (2015) 297–304, https://doi.org/10.1016/j.chemosphere.2014.11.062.

[16] S.K. Alharbi, W.E. Price, J. Kang, T. Fujioka, L.D. Nghiem, Ozonation of carbamazepine, diclofenac, sulfamethoxazole and trimethoprim and formation of major oxidation products, Desalin. Water Treat. 57 (2016) 29340–29351, https://doi.org/10.1080/19443994.2016.1172986.

[17] Y. Yang, X. Lu, J. Jiang, J. Ma, G. Liu, Y. Cao, W. Liu, J. Li, S. Pang, X. Kong, C. Luo, Degradation of sulfamethoxazole by UV, UV/H2O2 and UV/persulfate (PDS): Formation of oxidation products and effect of bicarbonate, Water Res. 118 (2017) 196–207, https://doi.org/10.1016/J.WATRES.2017.03.054.

[18] S. Agopcan Cinar, A. Ziylan-Yavaş, S. Catak, N.H. Ince, V. Aviyente, Hydroxyl radical-mediated degradation of diclofenac revisited: a computational approach to assessment of reaction mechanisms and by-products, Environ. Sci. Pollut. Res. Int. 24 (2017) 18458–18469, https://doi.org/10.1007/S11356-017-9482-7.

[19] B.C. Gilbert, J.R.L. Smith, M.S. Newton, J. Oakes, R.P. Prats, Azo dye oxidation with hydrogen peroxide catalysed by manganese 1,4,7-triazacyclononane complexes in aqueous solution, Org. Biomol. Chem. 1 (2003) 1568–1577, https://doi.org/10.1039/b301026k.

[20] A. Mirzaei, L. Yerushalmi, Z. Chen, F. Haghighat, J. Guo, Enhanced photocatalytic degradation of sulfamethoxazole by zinc oxide photocatalyst in the presence of fluoride ions: Optimization of parameters and toxicological evaluation, Water Res. 132 (2018) 241–251, https://doi.org/10.1016/J.WATRES.2018.01.016.

[21] A. Achilleos, E. Hapeshi, N.P. Xekoukoulotakis, D. Mantzavinos, D. Fatta-Kassinos, Factors affecting diclofenac decomposition in water by UV-A/TiO2 photocatalysis, Chem. Eng. J. 161 (2010) 53–59, https://doi.org/10.1016/j.cej.2010.04.020.

[22] A.A. Ameri, M. Shakibaie, M. Pournamdari, A.A. Ameri, A. Foroutanfar, M. Doostmohammadi, H. Forootanfar, Degradation of diclofenac sodium using UV/biogenic selenium nanoparticles/H_2O_2: Optimization of process parameters, J. Photochem. Photobiol. A: Chem. 392 (2020), https://doi.org/10.1016/j.jphotochem.2020.112382.

[23] H. Yu, E. Nie, J. Xu, S. Yan, W.J. Cooper, W. Song, Degradation of diclofenac by advanced oxidation and reduction processes: kinetic studies, degradation pathways and toxicity assessments, Water Res. 47 (2013) 1909–1918, https://doi.org/10.1016/j.watres.2013.01.016.

[24] S. Bae, D. Kim, W. Lee, Degradation of diclofenac by pyrite catalyzed Fenton oxidation, Appl. Catal. B: Environ. 134–135 (2013) 93–102, https://doi.org/10.1016/J.APCATB.2012.12.031.

[25] N. Farhadian, S. Liu, A. Asadi, M. Shahlaei, S. Moradi, Enhanced heterogeneous Fenton oxidation of organic pollutant via Fe-containing mesoporous silica composites: a review, J. Mol. Liq. 321 (2021), 114896, https://doi.org/10.1016/J.MOLLIQ.2020.114896.

[26] L. Clarizia, D. Russo, I. di Somma, R. Marotta, R. Andreozzi, Homogeneous photo-Fenton processes at near neutral pH: a review, Appl. Catal. B: Environ. 209 (2017) 358–371, https://doi.org/10.1016/J.APCATB.2017.03.011.

[27] Z. Wang, H. Shi, S. Wang, Y. Liu, Y. Fu, Degradation of diclofenac by Fe(II)-activated peracetic acid, Environ. Technol. (2020) 1–9, https://doi.org/10.1080/09593330.2020.1756926.

[28] T. Rodríguez-Álvarez, R. Rodil, J.B. Quintana, S. Triñanes, R. Cela, Oxidation of non-steroidal anti-inflammatory drugs with aqueous permanganate, Water Res. 47 (2013) 3220–3230, https://doi.org/10.1016/j.watres.2013.03.034.

[29] M.M. Sein, M. Zedda, J. Tuerk, T.C. Schmidt, A. Golloch, C. von Sonntag, Oxidation of diclofenac with ozone in aqueous solution, Environ. Sci. Technol. 42 (2008) 6656–6662, https://doi.org/10.1021/es8008612.

[30] D. Vogna, R. Marotta, A. Napolitano, R. Andreozzi, M. D'Ischia, Advanced oxidation of the pharmaceutical drug diclofenac with UV/H 2O2 and ozone, Water Res. 38 (2004) 414–422, https://doi.org/10.1016/j.watres.2003.09.028.

[31] X. Ao, W. Liu, W. Sun, C. Yang, Z. Lu, C. Li, Mechanisms and toxicity evaluation of the degradation of sulfamethoxazole by MPUV/PMS process, Chemosphere 212 (2018) 365–375, https://doi.org/10.1016/j.chemosphere.2018.08.031.

[32] J. Du, W. Guo, X. Li, Q. Li, B. Wang, Y. Huang, N. Ren, Degradation of sulfamethoxazole by a heterogeneous Fenton-like system with microscale zero-valent iron: Kinetics, effect factors, and pathways, J. Taiwan Inst. Chem. Eng. 81 (2017) 232–238, https://doi.org/10.1016/j.jtice.2017.10.017.

[33] W.Q. Guo, R.L. Yin, X.J. Zhou, J.S. Du, H.O. Cao, S.S. Yang, N.Q. Ren, Sulfamethoxazole degradation by ultrasound/ozone oxidation process in water: Kinetics, mechanisms, and pathways, Ultrason. Sonochem. 22 (2015) 182–187, https://doi.org/10.1016/j.ultsonch.2014.07.008.

[34] G. Ayoub, A. Ghauch, Assessment of bimetallic and trimetallic iron-based systems for persulfate activation: Application to sulfamethoxazole degradation, Chem. Eng. J. 256 (2014) 280–292, https://doi.org/10.1016/j.cej.2014.07.002.

[35] S. Gao, Z. Zhao, Y. Xu, J. Tian, H. Qi, W. Lin, F. Cui, Oxidation of sulfamethoxazole (SMX) by chlorine, ozone and permanganate-A comparative study, J. Hazard. Mater. 274 (2014) 258–269, https://doi.org/10.1016/j.jhazmat.2014.04.024.

[36] C. Qi, X. Liu, C. Lin, X. Zhang, J. Ma, H. Tan, W. Ye, Degradation of sulfamethoxazole by microwave-activated persulfate: Kinetics, mechanism and acute toxicity, Chem. Eng. J. 249 (2014) 6–14, https://doi.org/10.1016/j.cej.2014.03.086.

[37] A.G. Trovó, R.F.P. Nogueira, A. Agüera, A.R. Fernandez-Alba, C. Sirtori, S. Malato, Degradation of sulfamethoxazole in water by solar photo-Fenton. Chemical and toxicological evaluation, Water Res. 43 (2009) 3922–3931, https://doi.org/10.1016/j.watres.2009.04.006.

[38] R.F. Dantas, S. Contreras, C. Sans, S. Esplugas, Sulfamethoxazole abatement by means of ozonation, J. Hazard. Mater. 150 (2008) 790–794, https://doi.org/10.1016/j.jhazmat.2007.05.034.

[39] J. Eriksson, J. Svanfelt, L. Kronberg, A photochemical study of diclofenac and its major transformation products, Photochem. Photobiol. 86 (2010) 528–532, https://doi.org/10.1111/j.1751-1097.2009.00703.x.

[40] M. Rajab, G. Greco, C. Heim, B. Helmreich, T. Letzel, Serial coupling of RP and zwitterionic hydrophilic interaction LC-MS: suspects screening of diclofenac transformation products by oxidation with a boron-doped diamond electrode, J. Sep. Sci. 36 (2013) 3011–3018, https://doi.org/10.1002/jssc.201300562.

[41] C. Heim, M. Rajab, G. Greco, S. Grosse, J.E. Drewes, T. Letzel, B. Helmreich, Fate of diclofenac and its transformation and inorganic by-products in differentwater matrices during electrochemical advanced oxidation process using a boron-doped diamond electrode, Water 12 (2020), https://doi.org/10.3390/W12061686.

[42] A. Agüera, L.A. Perez Estrada, I. Ferrer, E.M. Thurman, S. Malato, A.R. Fernandez-Alba, Application of time-of-flight mass spectrometry to the analysis of phototransformation products of diclofenac in water under natural sunlight, J. Mass Spectrom. 40 (2005) 908–915, https://doi.org/10.1002/jms.867.

[43] L.A. Pérez-Estrada, S. Malato, W. Gernjak, A. Agüera, E.M. Thurman, I. Ferrer, A. R. Fernández-Alba, Photo-fenton degradation of diclofenac: Identification of main intermediates and degradation pathway, Environ. Sci. Technol. 39 (2005) 8300–8306, https://doi.org/10.1021/es050794n.

[44] K. Lekkerkerker-Teunissen, M.J. Benotti, S.A. Snyder, H.C. van Dijk, Transformation of atrazine, carbamazepine, diclofenac and sulfamethoxazole by low and medium pressure UV and UV/H2O2 treatment, Sep. Purif. Technol. 96 (2012) 33–43, https://doi.org/10.1016/j.seppur.2012.04.018.

[45] H. Yu, E. Nie, J. Xu, S. Yan, W.J. Cooper, W. Song, Degradation of diclofenac by advanced oxidation and reduction processes: kinetic studies, degradation pathways and toxicity assessments, Water Res. 47 (2013) 1909–1918, https://doi.org/10.1016/j.watres.2013.01.016.

[46] Z. Wang, H. Shi, S. Wang, Y. Liu, Y. Fu, Degradation of diclofenac by Fe(II)-activated peracetic acid, Environ. Technol. 42 (2021) 4333–4341, https://doi.org/10.1080/09593330.2020.1756926.

[47] G. Miyamoto, N. Zahid, J.P. Uetrecht, Oxidation of diclofenac to reactive intermediates by neutrophils, myeloperoxidase, and hypochlorous acid, Chem. Res. Toxicol. 10 (1997) 414–419, https://doi.org/10.1021/tx960190k.

[48] S. Othman, V. Mansuy-Mouries, C. Bensoussan, P. Battioni, D. Mansuy, Hydroxylation of diclofenac: an illustration of the complementary roles of biomimetic metalloporphyrin catalysts and yeasts expressing human cytochromes P450 in drug metabolism studies, Comptes Rendus De. l'Academie Des. Sci. - Ser. IIc: Chem. 3 (2000) 751–755, https://doi.org/10.1016/S1387-1609(00)01177-4.

[49] L. Zhang, Y. Liu, Y. Fu, Degradation kinetics and mechanism of diclofenac by UV/peracetic acid, RSC Adv. 10 (2020) 9907–9916, https://doi.org/10.1039/d0ra00363h.
[50] S. Chong, G. Zhang, N. Zhang, Y. Liu, T. Huang, H. Chang, Diclofenac degradation in water by FeCeOx catalyzed H2O2: Influencing factors, mechanism and pathways, J. Hazard. Mater. 334 (2017) 150–159, https://doi.org/10.1016/j.jhazmat.2017.04.008.
[51] M. del, M. Gómez-Ramos, M. Mezcua, A. Agüera, A.R. Fernández-Alba, S. Gonzalo, A. Rodríguez, R. Rosal, Chemical and toxicological evolution of the antibiotic sulfamethoxazole under ozone treatment in water solution, J. Hazard. Mater. 192 (2011) 18–25, https://doi.org/10.1016/j.jhazmat.2011.04.072.
[52] S. Willach, H. v Lutze, K. Eckey, K. Löppenberg, M. Lüling, J. Terhalle, J. B. Wolbert, M.A. Jochmann, U. Karst, T.C. Schmidt, Degradation of sulfamethoxazole using ozone and chlorine dioxide - compound-specific stable isotope analysis, transformation product analysis and mechanistic aspects, Water Res. 122 (2017) 280–289, https://doi.org/10.1016/j.watres.2017.06.001.
[53] M.C. Dodd, M.O. Buffle, U. von Gunten, Oxidation of antibacterial molecules by aqueous ozone: Moiety-specific reaction kinetics and application to ozone-based wastewater treatment, Environ. Sci. Technol. 40 (2006) 1969–1977, https://doi.org/10.1021/es051369x.
[54] S. Gao, Z. Zhao, Y. Xu, J. Tian, H. Qi, W. Lin, F. Cui, Oxidation of sulfamethoxazole (SMX) by chlorine, ozone and permanganate-A comparative study, J. Hazard. Mater. 274 (2014) 258–269, https://doi.org/10.1016/j.jhazmat.2014.04.024.
[55] M. Hong, Y. Wang, G. Lu, UV-Fenton degradation of diclofenac, sulpiride, sulfamethoxazole and sulfisomidine: Degradation mechanisms, transformation products, toxicity evolution and effect of real water matrix, Chemosphere 258 (2020), https://doi.org/10.1016/j.chemosphere.2020.127351.
[56] S. Poirier-Larabie, P.A. Segura, C. Gagnon, Degradation of the pharmaceuticals diclofenac and sulfamethoxazole and their transformation products under controlled environmental conditions, Sci. Total Environ. 557–558 (2016) 257–267, https://doi.org/10.1016/j.scitotenv.2016.03.057.
[57] C. Bellec, P. Maitte, J. Armand, C. Viel, Electrochemical reduction of nitroethylenic ketones in hydroorganic medium. Preparation of 4,5-dihydroxy-2-isoxazolines, Can. J. Chem. 59 (1981) 527–531, https://doi.org/10.1139/v81-074.
[58] M. Periša, S. Babić, I. Škorić, T. Frömel, T.P. Knepper, Photodegradation of sulfonamides and their N4-acetylated metabolites in water by simulated sunlight irradiation: kinetics and identification of photoproducts, Environ. Sci. Pollut. Res. 20 (2013) 8934–8946, https://doi.org/10.1007/s11356-013-1836-1.
[59] K. Kosaka, T. Nakai, Y. Hishida, M. Asami, K. Ohkubo, M. Akiba, Formation of 2,6-dichloro-1,4-benzoquinone from aromatic compounds after chlorination, Water Res. 110 (2017) 48–55, https://doi.org/10.1016/j.watres.2016.12.005.
[60] M. Bedner, W.A. MacCrehan, Transformation of acetaminophen by chlorination produces the toxicants 1,4-benzoquinone and N-acetyl-p-benzoquinone imine, Environ. Sci. Technol. 40 (2006) 516–522, https://doi.org/10.1021/es0509073.
[61] J.G.M. Bessems, N.P.E. Vermeulen, Paracetamol (Acetaminophen)-induced toxicity: molecular and biochemical mechanisms, Analog. Prot. Approaches 31 (2008) 55–138, https://doi.org/10.1080/20014091111677. ⟨Http://Dx.Doi.Org/10.1080/20014091111677⟩.
[62] M. Schmitt-Jansen, P. Bartels, N. Adler, R. Altenburger, Phytotoxicity assessment of diclofenac and its phototransformation products, Anal. Bioanal. Chem. 387 (2007) 1389–1396, https://doi.org/10.1007/s00216-006-0825-3.
[63] V. Osorio, J. Sanchís, J.L. Abad, A. Ginebreda, M. Farré, S. Pérez, D. Barceló, Investigating the formation and toxicity of nitrogen transformation products of diclofenac and sulfamethoxazole in wastewater treatment plants, J. Hazard. Mater. 309 (2016) 157–164, https://doi.org/10.1016/j.jhazmat.2016.02.013.
[64] J. Yang, G. Lv, C. Zhang, Z. Wang, X. Sun, Indirect photodegradation of sulfamethoxazole and trimethoprim by hydroxyl radicals in aquatic environment: mechanisms, transformation products and eco-toxicity evaluation, Int. J. Mol. Sci. 21 (2020) 1–14, https://doi.org/10.3390/IJMS21176276.
[65] G. v Nizova, C. Bolm, S. Ceccarelli, C. Pavan, G.B. Shul×pin, Hydrocarbon oxidations with hydrogen peroxide catalyzed by a soluble polymer-bound manganese(IV) complex with 1,4,7-triazacyclononane, Adv. Synth. Catal. 344 (2002) 899–905, https://doi.org/10.1002/1615-4169(200209)344:8.
[66] A. Grenz, S. Ceccarelli, C. Bolm, Synthesis and application of novel catalytically active polymers containing 1,4,7-triazacyclononanes, Chem. Commun. 1 (2001) 1726–1727, https://doi.org/10.1039/B105560G.